Research article

Journal of RAMAN SPECTROSCOPY

Received: 2 September 2016 Revised: 8 December 2016 Accepted: 10 December 2016 Published online in Wiley Online Library

(wileyonlinelibrary.com) DOI 10.1002/jrs.5094

Raman spectroscopy and imaging of Bernal-stacked bilayer graphene synthesized on copper foil by chemical vapour deposition: growth dependence on temperature

M. Fabiane,[a,b] M. J. Madito,[a] A. Bello[a] and N. Manyala[a]*

We report on the effect of temperature on the growth of bilayer graphene on a copper foil under atmospheric pressure chemical vapour deposition (AP-CVD). Before characterization of the AP-CVD bilayer graphene, a high-quality graphene flake was obtained from the Kish bulk graphite by micro-mechanical exfoliation and characterized by using Raman spectroscopy and imaging. The Raman data of the exfoliated, high-quality graphene flake show monolayer and bilayer graphenes and were compared with the Raman data of AP-CVD graphene. Raman spectroscopy of AP-CVD graphene shows bilayer films that exhibit predominantly Bernal stacking with an I_{2D}/I_G ratio of ~1. At low growth temperature (~780 °C), Raman disorder-related peak intensity in the AP-CVD graphene is high and decreases with an increase in growth temperature to the lowest disorder intensity at ~973 °C. The selected area electron diffraction and atomic force microscopy average step height analysis showed the thickness of the bilayer graphene. The AP-CVD graphene is uniform at low growth temperatures (~780 °C) with a high disorder and becomes non-uniform at high growth temperatures (~867–973 °C) with a very low disorder as bilayer graphene evolves to form islands with an average lateral size of <10 μm. Competition between carbon adatoms supply through dehydrogenation of the CH_x species, mobility and desorption rate of the carbon-adatom species for nucleation of the bilayer graphene as a function of temperature is elucidated. This study provides further insight into the growth mechanisms of bilayer graphene by AP-CVD on Cu.

Additional Supporting Information may be found online in the supporting information tab for this article.

Keywords: graphene; AP-CVD; copper foil; Bernal-stacked bilayer; exfoliated graphene

Introduction

Research has proven graphene synthesis by various methods such as the mechanical exfoliation of natural (Kish) graphite flakes and the transition metal-assisted chemical vapour deposition (CVD) that has shown unequivocal capacity to produce large-area graphene that has a potential use in transparent conducting electrodes,[1–4] supercapacitors[5–8] and integration with current complementary metal oxide semiconductor technology.[9–11] Although much time and effort have been applied to improve CVD graphene, most of the advances have been achieved primarily through empirical optimization of the growth parameters.[12] In CVD synthesis of graphene, Cu is a favourable catalyst due to its very low solubility of carbon (i.e. <0.001 at% at 1000 °C),[13] low cost and high etchability, and Cu typically grows a substrate size uniform monolayer graphene. However, CVD synthesis of uniform, defect-free (high quality) large-area bilayer and multilayer graphene on Cu substrate has proven to be more difficult. For instance, a CVD Bernal (AB)-stacked bilayer graphene synthesized on Cu only forms polycrystalline film consisting of discrete domains with a few micrometer size, although the interest is in achieving a large-area AB-stacked bilayer graphene.[14–18] The interest in AB-stacked bilayer graphene is motivated by its tunable bandgap of up to 250 mV when an external electric field is applied perpendicular to the two superimposed layers for practical applications such as graphene-based field-effect transistors.[19] The challenge of CVD synthesis of uniform, high-quality large-area bilayer and multilayer graphene on Cu substrate is ascribed primarily to the low decomposition rate of hydrocarbons on the Cu surface [partial dehydrogenation of the CH_x species (x = 1,2,3)].[14–16,20–22] In previous studies, atmospheric-pressure CVD (AP-CVD) was used to demonstrate a low hydrocarbon decomposition rate of Cu surface which was enhanced by alloying Cu with Ni to achieve a large-area (or substrate size) AB-stacked bilayer graphene.[23,24] However, the AP-CVD temperature dependence of AB-stacked bilayer graphene growth on Cu substrate was not investigated, and this study aims at such investigation. AP-CVD is a facile synthesis approach and allows high growth temperatures (below substrates melting points) without sublimation of substrates.

* *Correspondence to: Ncholu Manyala, Department of Physics, Institute of Applied Materials, SARChI Chair in Carbon Technology and Materials, University of Pretoria, Pretoria 0028, South Africa. E-mail: ncholu.manyala@up.ac.za*

a *Department of Physics, Institute of Applied Materials, SARChI Chair in Carbon Technology and Materials, University of Pretoria, Pretoria 0028, South Africa*

b *National University of Lesotho, Department of Physics and Electronics, P.O. Roma, Lesotho*

Furthermore, various methods are used to characterize the CVD graphene, and amongst these methods, Raman spectroscopy and imaging is a versatile, well-known reliable technique to study properties of graphene, for instance, to determine the number of graphene layers and the stacking order in few layers of graphene samples.[23,25–30] In this study, AP-CVD temperature dependence of AB-stacked bilayer graphene growth on Cu substrate was investigated. Raman spectroscopy and imaging was used to characterize the synthesized AP-CVD bilayer graphene. In the characterization of bilayer graphene, a high-quality graphene flake obtained from the Kish bulk graphite by micro-mechanical exfoliation by using scotch tape was characterized by using Raman spectroscopy and imaging, and the results consisted of monolayer and bilayer graphene as interpreted. The Raman data of the exfoliated graphene flake were compared with the Raman data of AP-CVD graphene. The Raman imaging/mapping, atomic force microscope (AFM) average step height analysis and the selected area electron diffraction (SAED) data showed that the as-grown graphene film is predominantly bilayer. Under the experimental conditions used in this study, the bilayer graphene does not fully evolve to cover the substrate at higher temperatures.

Experimental

For the AP-CVD temperature dependence of bilayer graphene growth, the temperature of the growth chamber was calibrated before graphene growth by using an adjustable thermocouple (chromel–alumel thermocouple, type K) inserted into the chamber so that the temperature could be measured at each centimetre from the highest temperature zone corresponding to the centre of the furnace [Fig. 1(a)]. The thermocouple of the furnace registered 918 °C at the tube centre, while the adjustable thermocouple read 973 °C at the highest temperature zone (centre of the tube furnace). In this study, the temperature reported is that of the adjustable thermocouple. During graphene synthesis, the temperature was first ramped up from room temperature to 1050 °C [measured at the highest temperature zone (centre) of the furnace] and was maintained at this temperature for 10 min in an Ar and H_2 atmosphere [Fig. 1(b)]. Thereafter, it was lowered to 973 °C, and a succession of temperature measurements was taken at each centimetre from the highest temperature zone by the adjustable thermocouple, as shown in Fig. 1(c). The thermocouple was moved from the highest temperature zone towards the low-temperature zone in steps of 1 cm, and the temperature was allowed to stabilize for 3 min at each new position before recorded. The 16-cm long Cu foil (25-μm thick foils, 99.8%, Alfa Aesar) was loaded into the quartz tube and placed along the length of one half of the furnace's heating elements so that it spanned the length of the element ~16 cm [see schematic in Fig. 1(a)]. In this way, the gas flow rate through the quartz tube was kept constant, while the temperature varied along the length of the Cu foil. In Fig. 1(c), it can be seen that temperature variation in 4 cm (~956–973 °C) and 8 cm (~939–956 °C) pieces of Cu foil is very small (±5 °C/cm) compared with 12 cm (~867–936 °C) and 16 cm (~780–862 °C) pieces which have a large temperature variation of ±25 °C/cm. Consequently, AP-CVD growth dependency on temperature was evaluated over a high-temperature zone (~939–973 °C) with small temperature variation and a low-temperature zone (~780–862 °C) with a large temperature variation. Graphene was synthesized by AP-CVD in a quartz tube furnace from a mixture of $Ar : CH_4 : H_2 = 300 : 10 : 9$ sccm gases on a Cu foil. The synthesis process and the growth temperature (measured at the highest temperature zone) are shown schematically and graphically in Fig. 1(a and b) respectively. After the graphene growth, the sample was rapidly cooled by pushing the quartz tube to the cooler part of the furnace and then was let to cool naturally to room temperature before it could be taken out of the tube.[31] The graphene was transferred onto 300-nm-thick

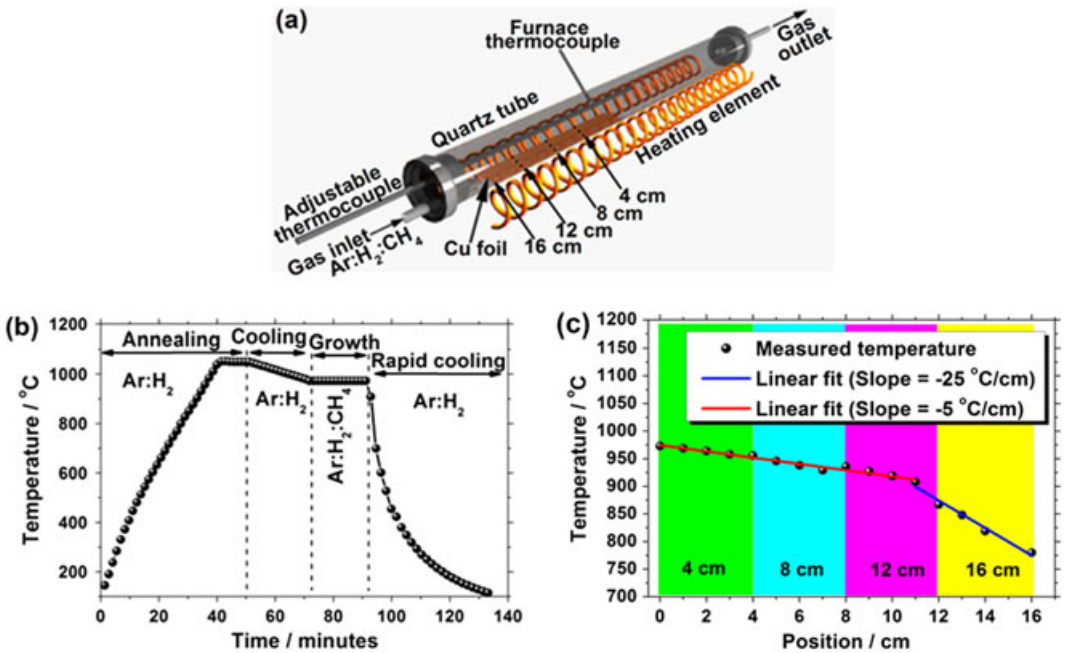

Figure 1. (a) Schematic diagram of the furnace tube showing a 16-cm long copper foil divided into four segments placed during graphene growth. (b) A temperature profile of AP-CVD system measured at the centre of a quartz tube by using adjustable thermocouple for the growth of graphene. (c) Temperature measurements taken at each centimetre from the centre of a quartz tube (973 °C) by the adjustable thermocouple. [Colour figure can be viewed at wileyonlinelibrary.com]

Journal of RAMAN SPECTROSCOPY

SiO_2/Si substrates and transmission electron microscopy (TEM) grids by spin coating a thin layer of polymethyl methacrylate on the as-grown graphene on Cu foil. For characterization of bilayer graphene obtained by using AP-CVD, high-quality graphene flakes were first obtained from the Kish bulk graphite by micro-mechanical exfoliation by using scotch tape and characterized for comparison with the AP-CVD graphene. The Raman data obtained from the exfoliated graphene flake are presented in the supporting information.

A T64000 micro-Raman spectrometer (HORIBA Scientific, Jobin Yvon Technology) with a 514-nm laser wavelength, 50× objective and a spectral acquisition time of 120 s was used to characterize the as-grown samples on the Cu foil and those transferred onto SiO_2/Si substrates. Raman imaging of the samples was carried out by using a WITec alpha 300R+ confocal Raman system (WITec GmbH) at 532-nm laser wavelength (2.33 eV) through a numerical aperture of 0.9 with a diffraction-limited spot size of 360 nm on the sample surface and 100 × magnifications, which allows an image spatial resolution of about 360 nm. A spectral resolution was 3 cm^{-1}, and the Raman system laser power was set as low as 1.6 mW in order to minimize heating effects. Electron diffraction pattern of graphene was obtained with high-resolution TEM (Jeol JEM-2100F field emission electron microscope, with a maximum analytical resolution of 200 kV and a probe size under 0.5 nm). The topographical image of graphene sample transferred onto the SiO_2/Si substrate was obtained by using a Dimension Icon AFM (Bruker AXS) with NANOSCOPE ANALYSIS software in Scan Asyst mode. The AFM cantilever with a spring constant of 2.8 N/m and a nominal resonance frequency of 75 kHz was used.

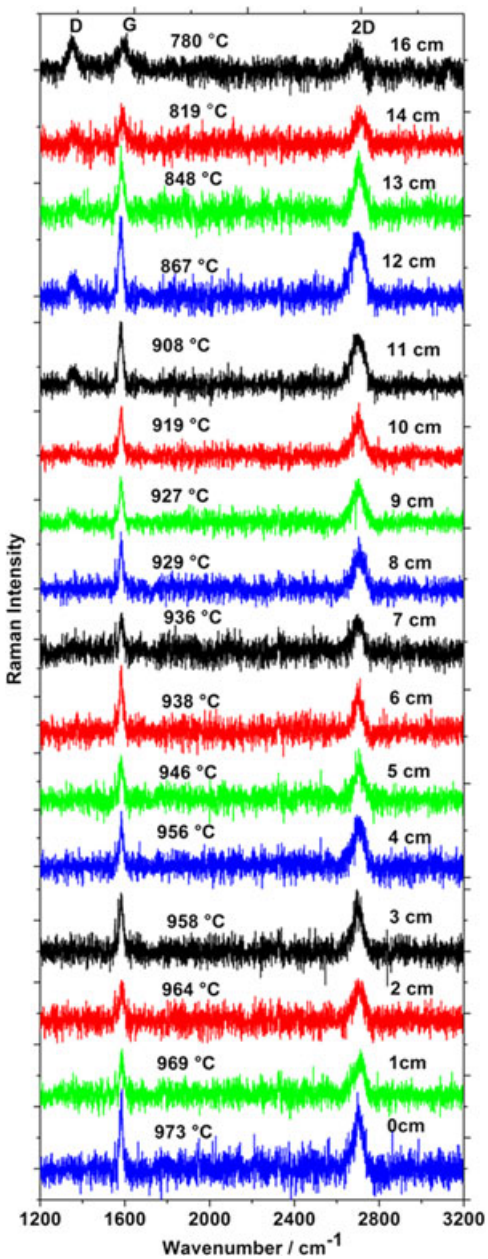

Figure 2. Raman spectra of as-grown bilayer graphene on 16-cm long Cu foil taken at intervals of 1 cm from the low-temperature region (~780 °C) to the high-temperature region (~973 °C) at the centre of the furnace. [Colour figure can be viewed at wileyonlinelibrary.com]

Results and discussions

In the AP-CVD graphene, the Raman spectra of the as-grown graphene were obtained directly from the 16-cm long Cu foil at intervals of 1 cm from the low-temperature region (~780 °C) to the high-temperature region (~973 °C) at the centre of the furnace, as shown in Fig. 2. Figure 2 shows the typical Raman spectra of as-

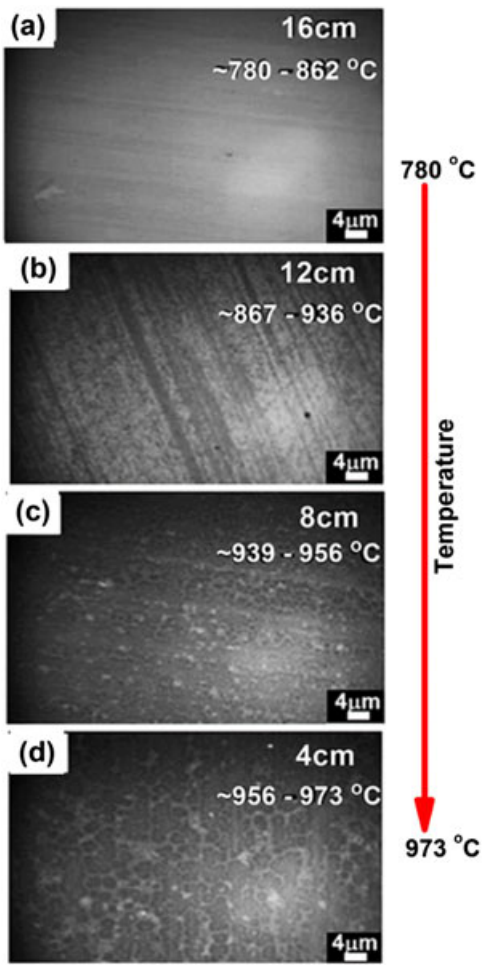

Figure 3. The optical micrographs of graphene samples transferred onto SiO_2/Si substrates corresponding to temperature ranges of (a) ~780–862 °C, (b) ~867–936 °C, (c) ~939–956 °C and (d) ~956–973 °C respectively. [Colour figure can be viewed at wileyonlinelibrary.com]

grown graphene on Cu foil after subtraction of Cu luminescent background by performing a background subtraction during the data analysis, and care was taken to ensure that the regions of the spectrum containing Raman peaks are not altered. For short acquisition time of good Raman spectra and imaging, as-grown graphene on Cu foil was transferred onto the SiO_2/Si substrate. The 16-cm long graphene/Cu foil was cut into four samples each 4 cm long and transferred onto SiO_2/Si substrates separately. Figure 3(a–d) shows the optical micrographs of each 4-cm long graphene samples transferred to SiO_2/Si substrates corresponding to temperature ranges of ~780–862 °C, ~867–936 °C, ~939–956 °C and ~956–973 °C. In the low-temperature range (~780–862 °C, 16 cm piece), the optical micrograph suggests a continuous graphene with a uniform thickness and at higher temperatures (~867–973 °C, 12 to 4-cm pieces); the graphene thickness varies as presented by each micrograph colour contrast because the optical micrograph displays the image colour contrast between monolayer and a few layer graphene. It was observed for exfoliated graphene flake that Raman imaging of the G mode displays the image colour contrast between monolayer and bilayer graphene [Fig. S1(c)]. Therefore, to confirm the thickness variation in the graphene samples, the Raman imaging of the G mode of each sample was obtained, as shown in Fig. 4.

In Fig. 4, at lower temperatures [~780–862 °C, 16-cm piece; Fig. 4(a)], the G mode imaging confirms a continuous graphene with a uniform thickness as indicated by optical micrograph. However, as temperature increases (~867–973 °C), a dark background (low G peak intensity regions) becomes clear as shown in the images of 12 to 4-cm pieces [Fig. 4(b–d)] which confirm non-uniform thickness in graphene obtained within the temperature range of these pieces. From the images, it can be seen that the few layer islands are clearly visible at the highest temperature of ~973 °C [Fig. 4(d)]. Additionally, the G peak intensities in the images of 12, 8 and 4-cm pieces (see the scale bar) are almost twice that of the 16-cm piece, suggesting that 12, 8 and 4-cm pieces are mostly comprised graphene with a thickness that is almost double that of the 16-cm piece because the G peak intensity follows a linear trend as the number of layers increases from mono to multilayer graphene, as mentioned in Fig. S1. Furthermore, Fig. 5 shows the mapping of the 2D-to-G peak intensity ratio (I_{2D}/I_G) which depicts that a 16-cm piece graphene has an I_{2D}/I_G of ~1 [blue-to-green colour in Fig. 5(a)] and 12, 8 and 4-cm piece graphene is mainly composed of I_{2D}/I_G of ~1 and small areas of I_{2D}/I_G of ~2 [yellow-to-red colour in Fig. 5(b–d)]. The I_{2D}/I_G of ~1 observed from the mapping corresponds to that observed from the Raman spectra in Figs 2 and S1 for exfoliated bilayer graphene,

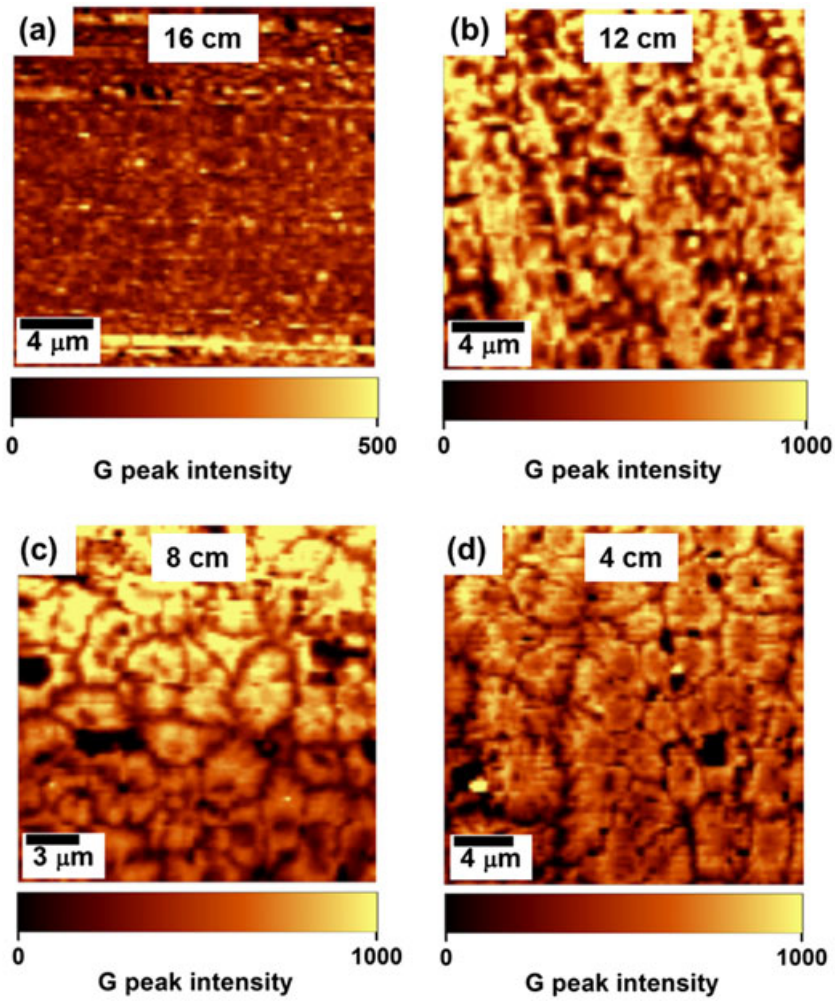

Figure 4. (a–d) Raman imaging of the G mode for the graphene samples [i.e. 16, 12, 8 and 4-cm pieces corresponding to temperature ranges of (a) ~780–862 °C, (b) ~867–936 °C, (c) ~939–956 °C and (d) ~956–973 °C respectively] transferred onto SiO_2/Si substrates. [Colour figure can be viewed at wileyonlinelibrary.com]

Journal of RAMAN SPECTROSCOPY

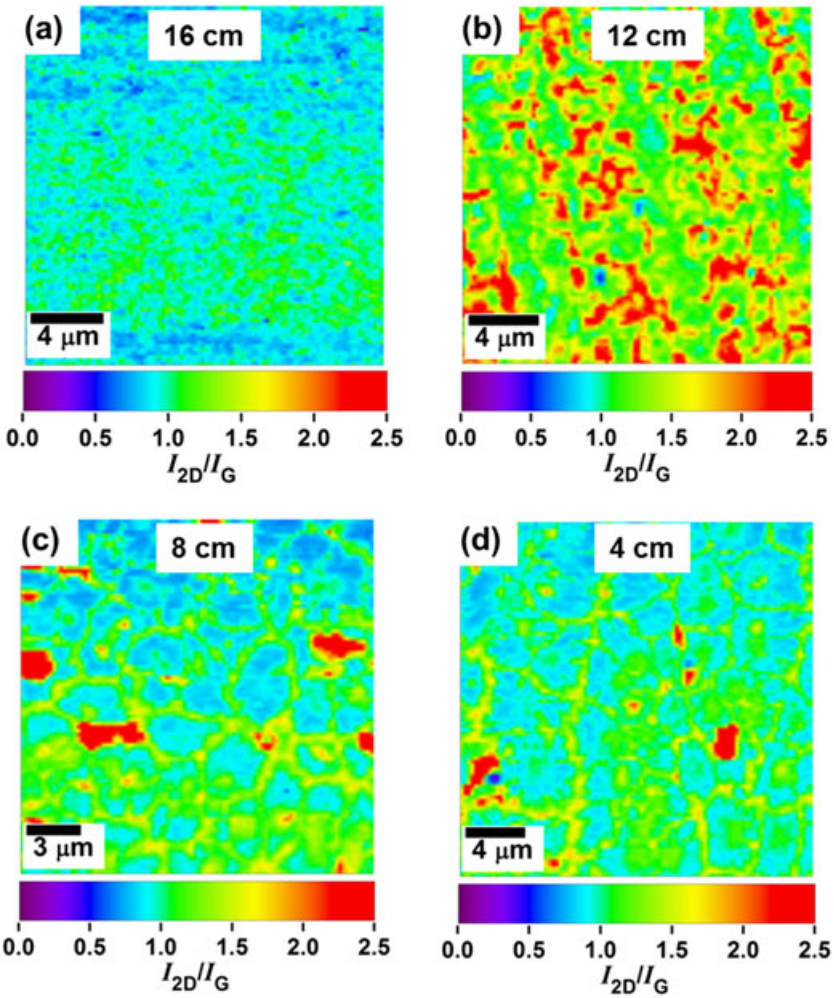

Figure 5. (a–d) Raman mapping of the 2D-to-G peak intensity ratio (I_{2D}/I_G) for the graphene samples [i.e. 16, 12, 8 and 4-cm pieces corresponding to temperature ranges of (a) ~780–862 °C, (b) ~867–936 °C, (c) ~939–956 °C and (d) ~956–973 °C respectively] transferred onto SiO_2/Si substrates. [Colour figure can be viewed at wileyonlinelibrary.com]

and this ratio suggests that the as-grown graphene is predominantly AB-stacked bilayer graphene.[32] In Fig. 5(b–d), small areas with I_{2D}/I_G of ~2 (yellow-to-red colour) correspond to darker areas in Fig. 4(b–d) which could be monolayer graphene.

Similar to exfoliated graphene flake, to determine the number of layers in the AP-CVD samples, the Raman spectra which show the D, G, D′ and 2D modes were obtained from each of the four samples in Fig. 4 [Fig. 6(a)]. In the samples, the calculated D-to-G peak intensity ratio increases with decreasing growth temperature [Fig. 6(b)], suggesting low-quality (or high disorder) graphene at low growth temperatures (<900 °C) and high-quality graphene at growth temperatures higher than 900 °C. The area under the D peak increases with decreasing growth temperature [Fig. 6(b)], suggesting an increase in the contribution of defects in graphene with a decrease in growth temperature which could be attributed to the partial dehydrogenation of the CH_x species (x = 1,2,3) due to low growth temperature and high background pressure of AP-CVD. Contrary to low-pressure CVD (LP-CVD) which has a lower density of impurities and residual gas due to high vacuum,[21] AP-CVD grows high-disorder graphene on Cu substrate at lower growth temperatures (<900 °C). However, at higher growth temperatures (~1000 °C), AP-CVD grows high-quality graphene. To determine the number of layers in the samples, the Lorentzian fits of the 2D mode were obtained [Fig. 6(c–e)] similar to that of exfoliated graphene flake [Fig. S1(e)]. The Lorentzian fits for graphene achieved at lower growth temperatures (~780–862 °C, 16-cm piece) were not obtained due to high disorder (high D peak intensity relative to G peak) which could influence the broadening of the 2D peak. However, it is worth mentioning that 2D mode originates from the double resonance process that involves two in-plane transverse optical mode phonons and is independent of defects; however, the D mode involves one in-plane transverse optical mode phonon and one defect.[33] In addition, the Lorentzian fit approach used to distinguish between the numbers of layers in graphene is adopted for high-quality graphene (i.e. low D peak intensity relative to G peak).[25,28] Similar to exfoliated graphene flake, the Lorentzian fits as well as the I_{2D}/I_G ratio of ~1 demonstrate characteristics of the AB-stacked bilayer graphene.[27,34]

Raman imaging of the 2D peak full width at half maximum (FWHM) and the corresponding FWHM line profile across the 2D peak FWHM image for the graphene samples show an average value of 55.3 cm^{-1} [Fig. 7(a and b) for 4-cm piece graphene at ~956–973 °C] which compares well with the average values 51,[35] 53[22] and 60.1 cm^{-1}[18] found in literature for AB-stacked bilayer graphene. The minimum average FWHM (32 cm^{-1}) in Fig. 7(b)

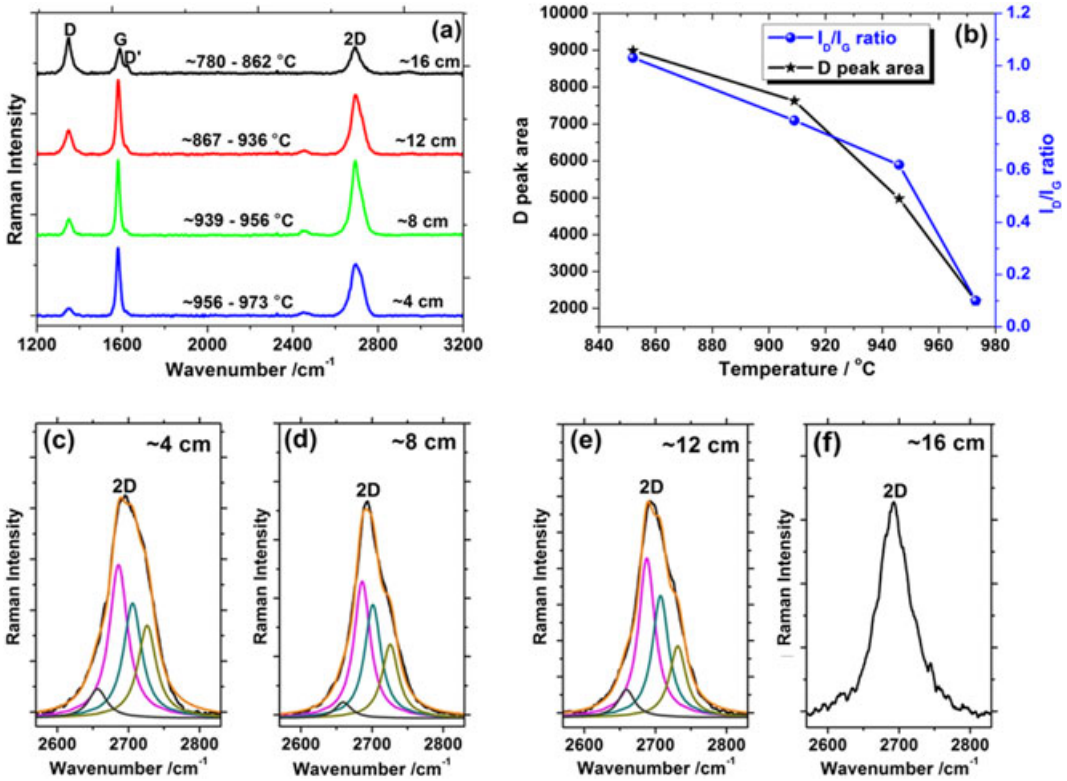

Figure 6. (a) Raman spectra of each of the graphene samples (i.e. 16, 12, 8 and 4-cm pieces corresponding to temperature ranges of ~780–862 °C, ~867–936 °C, ~939–956 °C and ~956–973 °C respectively) transferred onto SiO_2/Si substrates. (b) The area under D peak and the D-to-G peak intensity ratio of Raman spectra of each of the graphene samples. (c–f) The 2D mode of the Raman spectra in (a) and the corresponding Lorentzian fits. [Colour figure can be viewed at wileyonlinelibrary.com]

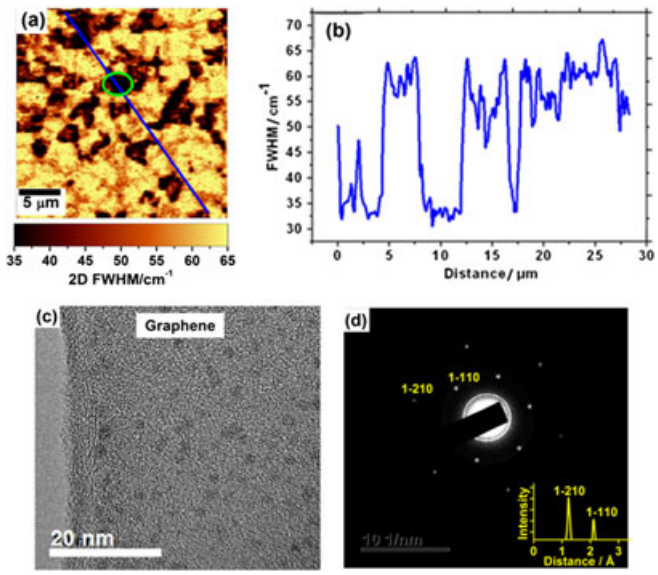

Figure 7. (a) Raman imaging of the 2D peak FWHM and (b) the corresponding FWHM line profile across the image in (a) for graphene of a 4-cm piece at ~956–973 °C. (c) A high-magnification TEM image for graphene of a 4-cm piece at ~956–973 °C and (d) the corresponding SAED pattern which shows the diffraction ring intensity profile (inset to the figure). [Colour figure can be viewed at wileyonlinelibrary.com]

corresponding to the dark areas (green circle) in Fig. 7(a) compares well with that of exfoliated graphene flake for monolayer graphene.

Figure 7(c and d) shows a high-magnification TEM image and SAED pattern respectively for graphene of a 4-cm piece at ~956–973 °C transferred on a TEM grid. A SAED pattern shows two sets of hexagonal diffraction spots and the corresponding intensity profile [inset to Fig. 7(d)] taken along the inner and outer diffraction rings which were indexed by using the Miller–Bravais indices (*hkl*) for graphite where peaks at $d = 1.23$ and 2.13 Å correspond to indices (1–210) for outer hexagon and (1–110) for inner hexagon respectively.[36] An intensity profile [inset to Fig. 7(d)] shows that the intensity of the diffraction spots in the outer hexagon is twice the intensity of the diffraction spots in the inner hexagon, indicating that the set of diffraction spots corresponds to an AB-stacked bilayer graphene. Figure 8(a) shows an AFM optical microscope image (showing AFM cantilever and graphene film) for graphene of a 4-cm piece at ~956–973 °C transferred onto SiO_2/Si substrate. In Fig. 8(b), the AFM image of graphene film shows the edge and wrinkles of the graphene sheet shown in Fig. 8(a). From the edge of the graphene film [i.e. from Si/SiO_2 to graphene film along the solid line in Fig.8 (b)], the height profile was measured, as shown in Fig. 8(c), which depicts that the thickness of the graphene film has an average value of about 1.5 nm, suggesting bilayer graphene.

In summary, the optical micrographs and the Raman imaging/mapping for graphene samples obtained from 12, 8 and 4-cm pieces corresponding to temperature ranges of ~867–936 °C, ~939–956 °C and ~956–973 °C respectively (Figs 3–5) display growth of graphene which is predominantly AB-stacked bilayer. The SAED and AFM step height analysis confirmed the thickness of the bilayer graphene. The observed islands of bilayer graphene (dark areas in optical micrographs) are part of a continuous monolayer graphene (light areas in optical micrographs). Therefore, because the growth of bilayer graphene is evident from growth temperatures in the range of ~867–973 °C (12 to 4-cm

Journal of RAMAN SPECTROSCOPY

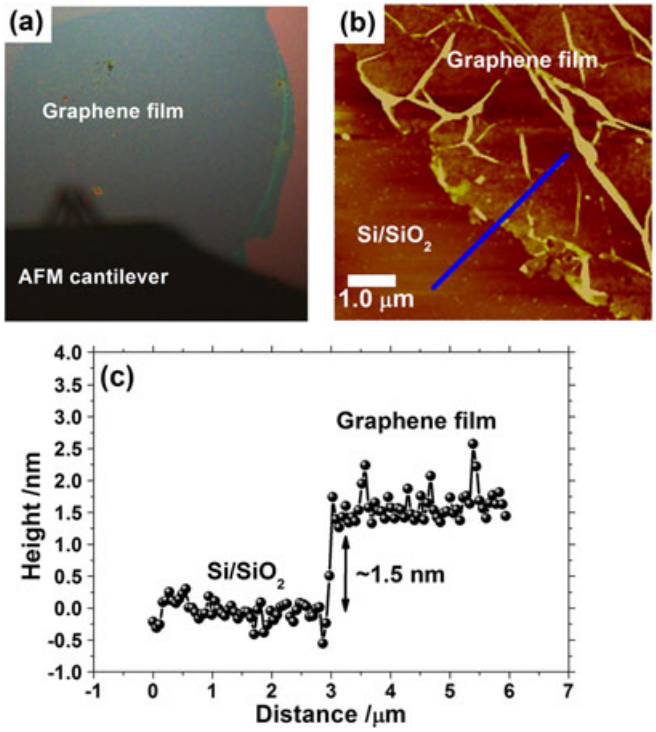

Figure 8. (a) AFM optical microscope image (showing AFM cantilever and graphene film). (b) AFM image of graphene film showing the edge and wrinkles of the sheet. (c) Height profile measured along the solid line in (b). [Colour figure can be viewed at wileyonlinelibrary.com]

pieces) and the light areas (monolayer graphene) in optical micrographs of 12 to 4-cm pieces compare well with 16-cm piece optical micrograph, it can be mentioned that a continuous graphene with a uniform thickness observed from the optical micrographs and the Raman imaging/mapping at growth temperatures in the range of ~780–862 °C (16-cm piece) is predominantly high-disorder monolayer graphene. The high disorder of this graphene could be attributed to the partial dehydrogenation of the CH_x species ($x = 1,2,3$) at low AP-CVD growth temperatures presumably because Cu is known to have low decomposition rate of methane gas.[20,21,37] In addition, the high disorder (high D peak intensity) of this graphene could increase the intensity of the G peak through D′ peak [G peak right-shoulder shown in Fig. 6(a)] which is supposed to be less relative to 2D peak for monolayer compared with bilayer graphene as demonstrated by Raman imaging of G mode for exfoliated graphene flake. The high disorder could also contribute to the broadening of the 2D peak, resulting in FWHM range (48–71 cm^{-1}) similar to that of high-quality (low D peak intensity) bilayer graphene (Fig. S2).

To explain the dendritic behaviour of graphene domains observed under the AP-CVD growth for graphene of a 4-cm piece at ~956–973 °C, the mechanism proposed by Li *et al.*[38] was adopted. The mechanism suggests that the limited space in the interface between the top graphene layer and the Cu substrate forms a 'nano-CVD' chamber. The extreme physical confinements in the nano-CVD chamber result in a lower partial pressure of CH_x species, which manifests in a decreased growth rate. The non-uniformity of precursor distribution in the deposition chamber under AP-CVD is eliminated by the confined space between the top graphene layer and the Cu catalyst and hence the growth mimics that of LP-CVD having domains with dendritic appearance resulting from underlayer of a bilayer graphene.[32,39–41]

The dependence of graphene domain size on temperature is elucidated by adopting the model and the experimental results of Kim *et al.*[12,42] In this model, the occurrence of two nucleation regimes is a result of the competition among the processes of adatom capture, surface diffusion and desorption.[12,42] In the low-temperature regime, desorption of carbon adatoms is negligible due to its high-activation barrier[12,37] and carbon surface diffusion determines the growth. In the high-temperature regime, desorption is a dominant process and hence the domain growth may be hindered depending on the gas supply. The mechanism was adopted based on the growth of a monolayer graphene, whereas it is applied to bilayer graphene growth in this work; our experimental results are in good agreement with it when the so-called underlayer growth mechanism in multilayer graphene is considered.[17,31,43] In the underlayer growth mechanism of multilayers, the subsequent layers grow beneath the top monolayer.[17,31,43] However, such a structure should form at suitably higher temperatures[38]; in this regime, the top layer grows faster and becomes larger than the second layer. This is a desorption-controlled regime.[12] The capture probability of carbon atoms is expected to be higher for the top layer than for the underlayer because the C atoms first have to pass the edge of the top layer and penetrate under it to the growing underlayer. Carbon atoms are captured on the way, and few adatoms may reach the bottom layer; hence, the top layer grows faster. In the low-temperature regime, desorption is negligible due to the high-activation energy barrier and adatom mobility controls the nucleation.[12] In this way, both the top and bottom layers should have a sufficient supply of carbon adatoms to grow and fully cover the substrate. However, in this work, in the low-temperature range of ~780–867 °C, a Cu catalyst shows a high-disorder graphene which could be attributed to the partial dehydrogenation of the CH_x species which would lead to insufficient supply of C adatoms required for high-quality substrate-size bilayer graphene. In contrast to low-temperature range, in a high-temperature range of ~956–973 °C, high-quality bilayer graphene islands with an average lateral size of <10 μm are evident, suggesting that for bilayer graphene growth on Cu catalyst, a CVD growth temperature higher than 900 °C is essential. Nonetheless, in the model and the experimental results of Kim *et al.*,[12,42] it is clearly demonstrated that for substrate-size graphene to grow on a Cu catalyst, the CVD growth temperature should be approximately 1000 °C.

Conclusions

We have elucidated the role of temperature in the synthesis of AB-stacked bilayer graphene on Cu foil. For our growth parameters, the graphene grown at low temperature (~780–867 °C) is uniform, with a high disorder, while the graphene grown at a higher temperature (~956–973 °C) manifests predominantly as high-quality AB-stacked bilayer graphene islands with an average lateral size of <10 μm and does not fully evolve to cover the substrate except for the top monolayer graphene. This is ascribed to the competition among carbon adatom supply through dehydrogenation of the CH_x species, mobility and desorption of carbon adatoms during the graphene growth. The dendritic growth similar to the growth under LP-CVD is ascribed to the confined space between the top graphene layer and the Cu catalyst which eliminates the non-uniform distribution of precursors in the AP-CVD graphene growth.

Acknowledgements

This study is based on research supported by the South African Research Chairs Initiative of the South Africa Department of Science and Technology and the National Research Foundation (NRF) (grant no. 97994). Any opinions, findings and conclusions or recommendations expressed in this study are those of the authors and therefore the NRF and Department of Science and Technology do not accept any liability with regard thereto. MF thanks the University of Pretoria and the NRF for financial support during his PhD studies.

References

[1] K. S. Kim, Y. Zhao, H. Jang, S. Y. Lee, J. M. Kim, K. S. Kim, J.-H. Ahn, P. Kim, J.-Y. Choi, B. H. Hong, *Nature* **2009**, *457*, 706.
[2] X. Li, Y. Zhu, W. Cai, M. Borysiak, B. Han, D. Chen, R. D. Piner, L. Colombo, R. S. Ruoff, *Nano Lett.* **2009**, *9*, 4359.
[3] S. Bae, H. Kim, Y. Lee, X. Xu, J.-S. Park, Y. Zheng, J. Balakrishnan, T. Lei, H. Ri Kim, Y. Il Song, Y.-J. Kim, K. S. Kim, B. Özyilmaz, J.-H. Ahn, B. H. Hong, S. Iijima, *Nat. Nanotechnol.* **2010**, *5*, 574.
[4] D. Dodoo-arhin, M. Fabiane, A. Bello, N. Manyala, *Ind. Eng. Chem. Res.* **2013**, *52*, 14160.
[5] J. Xia, F. Chen, J. Li, N. Tao, *Nat. Nanotechnol.* **2009**, *4*, 505.
[6] Z.-S. Wu, K. Parvez, X. Feng, K. Mullen, *Nat. Commun.* **2013**, *4*, 2487.
[7] A. Bello, M. Fabiane, D. Dodoo-Arhin, K. I. Ozoemena, N. Manyala, *J. Phys. Chem. Solid* **2014**, *75*, 109.
[8] A. Bello, O. O. Fashedemi, J. N. Lekitima, M. Fabiane, D. Dodoo-arhin, Y. Gogotsi, A. T. C. Johnson, N. Manyala, *AIP Adv.* **2013**, *3*, 82118.
[9] K. S. Novoselov, A. K. Geim, S. V. Morozov, D. Jiang, Y. Zhang, S. V. Dubonos, I. V. Grigorieva, A. A. Firsov, *Science* **2004**, *306*, 666.
[10] Y.-M. Lin, C. Hsin-Ying, K. A. Jenkins, D. B. Farmer, P. Avouris, A. Valdes-Garcia, *Electron Device Lett. IEEE* **2010**, *31*, 68.
[11] F. Xia, D. B. Farmer, Y.-M. Lin, P. Avouris, *Nano Lett.* **2010**, *10*, 715.
[12] H. Kim, C. Mattevi, M. R. Calvo, J. C. Oberg, L. Artiglia, S. Agnoli, C. F. Hirjibehedin, M. Chhowalla, E. Saiz, *ACS Nano* **2012**, *6*, 3614.
[13] G. A. López, E. J. Mittemeijer, *Scr. Mater.* **2004**, *51*, 1.
[14] A. Guermoune, T. Chari, F. Popescu, S. S. Sabri, J. Guillemette, H. S. Skulason, T. Szkopek, M. Siaj, *Carbon* **2011**, *49*, 4204.
[15] W. Liu, H. Li, C. Xu, Y. Khatami, K. Banerjee, *Carbon* **2011**, *49*, 4122.
[16] A. Mohsin, L. Liu, P. Liu, W. Deng, I. N. Ivanov, G. Li, O. E. Dyck, G. Duscher, J. R. Dunlap, K. Xiao, G. Gu, *ACS Nano* **2013**, *7*, 8924.
[17] S. Nie, W. Wu, S. Xing, Q. Yu, J. Bao, S. Pei, K. F. McCarty, *New J. Phys.* **2012**, *14*, 93028.
[18] W. Fang, A. L. Hsu, R. Caudillo, Y. Song, A. G. Birdwell, E. Zakar, M. Kalbac, M. Dubey, T. Palacios, M. S. Dresselhaus, P. T. Araujo, J. Kong, *Nano Lett.* **2013**, *13*, 1541.
[19] Y. Zhang, T. Tang, C. Girit, Z. Hao, M. C. Martin, A. Zettl, M. F. Crommie, Y. R. Shen, F. Wang, *Nature* **2009**, *459*, 820.
[20] S. Bhaviripudi, X. Jia, M. S. Dresselhaus, J. Kong, *Nano Lett.* **2010**, *10*, 4128.
[21] W. Liu, S. Kraemer, D. Sarkar, H. Li, P. M. Ajayan, K. Banerjee, *Chem. Mater.* **2014**, *26*, 907.
[22] S. Chen, W. Cai, R. D. Piner, J. W. Suk, Y. Wu, Y. Ren, J. Kang, R. S. Ruoff, *Nano Lett.* **2011**, *11*, 3519.
[23] M. J. Madito, A. Bello, J. K. Dangbegnon, C. J. Oliphant, W. A. Jordaan, T. M. Masikhwa, D. Y. Momodu, N. Manyala, *J. Raman Spectrosc.* **2016**, *47*, 553.
[24] M. J. Madito, N. Manyala, A. Bello, J. K. Dangbegnon, T. M. Masikhwa, D. Y. Momodu, *RSC Adv.* **2016**, *6*, 28370.
[25] A. C. Ferrari, D. M. Basko, *Nat. Nanotechnol.* **2013**, *8*, 235.
[26] Y. Hao, Y. Wang, L. Wang, Z. Ni, Z. Wang, R. Wang, C. K. Koo, Z. Shen, J. T. L. Thong, *Small* **2010**, *6*, 195.
[27] L. M. Malard, M. A. Pimenta, G. Dresselhaus, M. S. Dresselhaus, *Phys. Rep.* **2009**, *473*, 51.
[28] A. C. Ferrari, J. C. Meyer, V. Scardaci, C. Casiraghi, M. Lazzeri, F. Mauri, S. Piscanec, D. Jiang, K. S. Novoselov, S. Roth, A. K. Geim, *Phys. Rev. Lett.* **2006**, *97*, 187401.
[29] J. M. Caridad, F. Rossella, V. Bellani, M. S. Grandi, E. Diez, *J. Raman Spectrosc.* **2011**, *42*, 286.
[30] J. M. Caridad, F. Rossella, V. Bellani, M. Maicas, M. Patrini, E. Díez, *J. Appl. Phys.* **2010**, *108*, 84321.
[31] M. Fabiane, S. Khamlich, A. Bello, J. Dangbegnon, D. Momodu, A. T. Charlie Johnson, N. Manyala, *AIP Adv.* **2013**, *3*, 112126.
[32] L. Liu, H. Zhou, R. Cheng, W. J. Yu, Y. Liu, Y. Chen, J. Shaw, X. Zhong, Y. Huang, X. Duan, *ACS Nano* **2012**, *6*, 8241.
[33] H. Aoki, M. S. Dresselhaus (Eds), *Physics of Graphene*, Springer, New York, **2014**.
[34] A. C. Ferrari, *Solid State Commun.* **2007**, *143*, 47.
[35] S. Lee, K. Lee, Z. Zhong, *Nano Lett.* **2010**, *10*, 4702.
[36] A. Dato, V. Radmilovic, Z. Lee, J. Phillips, M. Frenklach, *Nano Lett.* **2008**, *8*, 2012.
[37] W. Zhang, P. Wu, Z. Li, J. Yang, *J. Phys. Chem. C* **2011**, *115*, 17782.
[38] Q. Li, H. Chou, J. Zhong, J. Liu, A. Dolocan, J. Zhang, Y. Zhou, R. S. Ruo, S. Chen, W. Cai, *Nano Lett.* **2013**, *13*, 486.
[39] P. Zhao, A. Kumamoto, S. Kim, X. Chen, B. Hou, S. Chiashi, E. Einarsson, Y. Ikuhara, S. Maruyama, *J. Phys. Chem. C* **2013**, *117*, 10755.
[40] X. Li, C. W. Magnuson, A. Venugopal, R. M. Tromp, J. B. Hannon, E. M. Vogel, L. Colombo, R. S. Ruo, *J. Am. Chem. Scociety* **2011**, *133*, 2816.
[41] Y. Zhang, L. Zhang, P. Kim, M. Ge, Z. Li, C. Zhou, *Nano Lett.* **2012**, *12*, 2810.
[42] V. N. E. Robinson, J. L. Robins, *Thin Solid Films* **1974**, *20*, 155.
[43] A. Y. Tontegode, *Prog. Surf. Sci.* **1991**, *38*, 201.

Supporting information

Additional Supporting Information may be found online in the supporting information tab for this article.